

RESEARCH ARTICLE | FEBRUARY 27 2007

Determining the absolute efficiency of a delay line microchannel-plate detector using molecular dissociation

B. Gaire; A. M. Sayler; P. Q. Wang; Nora G. Johnson; M. Leonard; E. Parke; K. D. Carnes; I. Ben-Itzhak

 Check for updates

Rev. Sci. Instrum. 78, 024503 (2007)

<https://doi.org/10.1063/1.2671497>



View
Online



Export
Citation

CrossMark

Articles You May Be Interested In

Absolute detection efficiency of a microchannel plate detector for neutral atoms

Rev Sci Instrum (May 2000)

Improved ion detection efficiency of microchannel plate detectors

Rev Sci Instrum (March 2002)

Absolute detection efficiency of a microchannel plate detector for kilo-electron volt energy ions

Rev Sci Instrum (November 1999)

500 kHz or 8.5 GHz?
And all the ranges in between.

Lock-in Amplifiers for your periodic signal measurements



Find out more

 Zurich
Instruments

Determining the absolute efficiency of a delay line microchannel-plate detector using molecular dissociation

B. Gaire, A. M. Sayler, P. Q. Wang,^{a)} Nora G. Johnson, M. Leonard, E. Parke, K. D. Carnes, and I. Ben-Itzhak

J. R. Macdonald Laboratory, Department of Physics, Kansas State University, Manhattan, Kansas 66506

(Received 30 June 2006; accepted 21 January 2007; published online 27 February 2007)

We present a method to measure the absolute detection efficiency of a delay-line microchannel-plate detector using the breakup of diatomic molecular ions. This method provides the absolute total detection efficiency, as well as the individual efficiency for each signal of the detector. The method is based on the fact that molecular breakup always yields two hits on the detector, but due to finite detection efficiency some of these events are recorded as single particles while others are detected in pairs. We demonstrate the method by evaluating the detection efficiency for both timing and position signals of a delay-line detector using laser-induced dissociation of molecular ions. In addition, the detection efficiency as a function of position has been determined by dividing the detector into sectors. © 2007 American Institute of Physics. [DOI: 10.1063/1.2671497]

I. INTRODUCTION

Measuring the detector efficiency, either absolute or relative, is an important task of instrumentation in science, as it enables the conversion of the measured counts to some useful quantity such as reaction probability or cross section. The absolute detection efficiency of a particle detector is defined as the probability that an incident particle will lead to a detected amplified output signal.

Detectors vary according to the nature of the particles or radiation detected. One of the most frequently used particle detectors, which has been used for ion, atom, electron, and photon detection, is the microchannel-plate (MCP) detector (see, for example, Refs. 1–5). A MCP works by the process of secondary electron emission to produce a charge pulse, in a similar way to channel electron multipliers (CEMs),^{6–8} and it has the desirable properties of high gain and high spatial and temporal resolution.⁹ In order to increase the number of secondary electrons, a MCP contains many independent coated glass capillaries of very small diameter known as channels, which are slightly tilted with respect to the MCP face (see Ref. 9 for details). A hit on a MCP channel will generate a pulse of electrons at the output, which is then collected using an anode, e.g., a delay line in our case.

The detection efficiency of a MCP for incident charged particles is relatively high (~50% for our detector), and it depends mainly on the following factors: (i) open-area-ratio (OAR)—The OAR is the ratio of the open area of the channels to the total effective area of the MCP. In general, it is more than 50%. (ii) Bias angle—The channel bias angle is the angle formed by the channel axis and the vertical axis to the plate surface. (iii) Bias voltage—The voltage drop across the channel plate which determines the charge gain. (iv) Recovery time—The minimum time difference required be-

tween two hits such that the detector is ready to register the later hit.^{9–14} It has been shown that the detection efficiency also depends on the incident particle energy and mass,^{12–18} especially for low energy particles, and to a lesser extent on the impact angle on the detector face.¹¹ Careful setting of the readout electronics, such as discriminator levels, will also affect the overall detection efficiency.⁴ Therefore, the detection efficiency is not just the OAR of the MCP,¹⁹ though usually it is about that value when charge saturation is achieved.^{19–21}

The detection efficiency can be increased beyond the OAR by using an electric field in front of the input plate, which redirects some of the secondary electrons emitted backward (especially by particles impacting on the “glass web”) into the active MCP channels.^{22–25} The resulting increase in detection efficiency plays an important role in many applications.

A delay line anode MCP detector is used in our experimental studies of laser and molecular-ion beam interactions using coincidence (3D) three-dimensional momentum imaging.^{26,27} This anode can handle a high counting rate with the good temporal and spatial resolution needed in such imaging experiments. Details on the performance of the MCPs with delay-line anodes can be found in the literature (see, for example, Refs. 14 and 28–30). It is important to note that in such coincidence experiments the particles hit the detector a short time after one another, thus signals might be lost due to the dead time of the constant fraction discriminator (CFD) used to pick the signals, resulting in a reduced detection efficiency.

In this article, we describe an experimental method to determine the absolute detection efficiency, which takes advantage of the fact that molecular dissociation always leads to two particles hitting the detector in coincidence. Due to the finite detection efficiency, however, single hits are detected in addition to the pairs. This method does not require a comparison of the detection rate to a beam current mea-

^{a)}Present address: Department of Physics, Western Illinois University, Macomb, IL 61455.

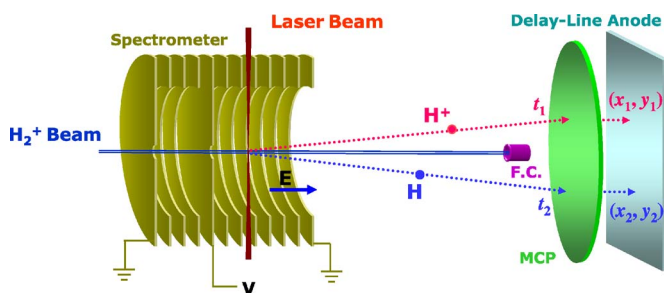


FIG. 1. Schematic representation of the experimental setup for laser-molecular ion interaction studies. The interaction occurs within the spectrometer. The fragments are detected by the time and position sensitive detector while the ion beam is collected in a small Faraday cup (F.C.).

surement as most previous methods do (see, for example, Refs. 10 and 17). To demonstrate the application of this method, we present results for the measured overall absolute detection efficiency (i.e., the total probability for detecting all signals of the incident particle), the absolute detection efficiency for individual position or time signals, and the position dependent efficiency for a delay-line detector. In addition, we show the usefulness of this method in the process of improving the detection efficiency. As our aim is to present this new technique, we have set the bias voltage of the detector below saturation, in the regime where small changes in voltage yield significant efficiency changes.^{9–13} Therefore, our results should be considered as an example of the method and not as an indicator of the capabilities of MCP detectors.

II. EXPERIMENT

The experimental arrangement for the detection efficiency measurement is shown in Fig. 1 and described in detail in our previous papers.^{26,27} The molecular ion beam is dissociated by a pulsed intense laser, and the fragments are then detected by a delay-line MCP detector down stream. The laser polarization is parallel to the detector plane. The delay line anode has four position signals which we label left (*L*), right (*R*), up (*U*), and down (*D*) in addition to a timing (*T*) signal picked up from the MCP front plate (there is no electric field in front of our MCP front plate). The physical characteristics of the MCP used in our experiments can be found in Ref. 31.

We are using homonuclear as well as heteronuclear molecular-ion beams in our experiments. Although we have shown the dissociation of a H_2^+ molecular ion in Fig. 1, the diagram is equally valid for a HD^+ beam. Molecular ions from an ion source are guided toward the spectrometer and finally to the Faraday cup. We use a beam energy of 7 keV and a spectrometer voltage of 1 kV. The voltage in the interaction region is 80% of the spectrometer voltage. Energies of the H, H^+ , D, and D^+ fragments upon impact on the detector are 2.06, 2.86, 4.13, and 4.93 keV, respectively. Here the neutrals have the same energy as that in the interaction region, but the charged particles have an extra energy corresponding to the spectrometer acceleration. An ultrashort intense laser pulse is incident on the molecular beam so that dissociation and ionization occur in the interaction region.

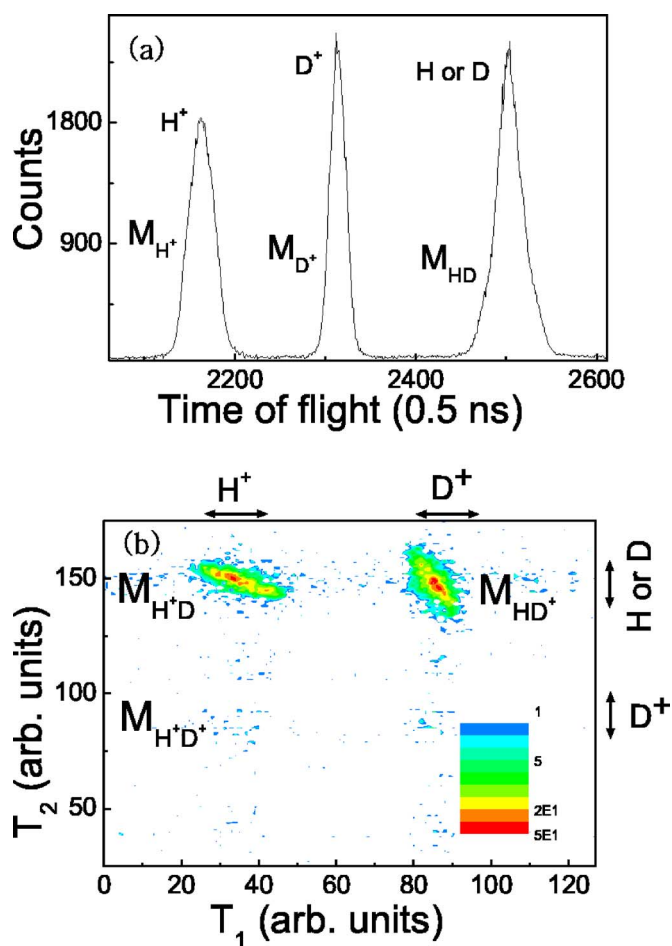


FIG. 2. (a) Measured number of detected hits as a function of TOF. (b) Coincidence TOF spectra presented as a density plot.

Because of the spectrometer voltage, the resulting fragments (ions and neutrals) hit the detector at different times. The resulting time-of-flight (TOF) spectra are analyzed to get the measured number of detected hits (i.e., all hits detected independent of whether or not the other hit is detected) and coincidences (i.e., fragment pairs detected). In our experiments, the counting rate is kept low enough to ensure that the random coincidence rate is negligible.

The number of detected hits is measured from the TOF spectrum shown in Fig. 2(a). It is important to note that the shortest time separation between fragments of one molecule is 60 ns (a backward D^+ in coincidence with a forward H), which is controlled by the strength of the electric field produced by the spectrometer. This time separation is much longer than the dead time of the CFD (≈ 10 ns) we used. Furthermore, the multihit electronics allow us to record all the signals in a pulse train. Therefore no signals are lost due to time overlap. The neutral fragments have the same TOF and hence are indistinguishable. The measured number of detected hits is given by the background-subtracted area under each peak. Thus, M_{H^+} , M_{D^+} , and M_{HD} are the measured number of detected hits for H^+ , D^+ , and neutral fragments, respectively.

The number of coincidences is measured from the coincidence TOF spectra, shown in Fig. 2(b). Here $M_{\text{H}^+\text{D}}$, M_{HD^+} , and $M_{\text{H}^+\text{D}^+}$ are the measured number of coincidences for the

dissociation channels $H^+ + D$ and $H + D^+$, and the ionization channel $H^+ + D^+$, respectively, to be discussed later. To analyze the coincidence TOF spectrum, we first rotate the spectrum of each channel such that the resulting distribution is horizontal and then project along one of the axes. Finally, we evaluate the background-subtracted area under the resulting peak. For simplicity, we have chosen an experimental data set without ionization (i.e., $M_{H^+D^+} \approx 0$).

III. ABSOLUTE EFFICIENCY EVALUATION

In this method, the efficiency of the detector is evaluated from the ratio of the measured coincidences to detected hits as explained below. This method is applicable when the molecular breakup always produces two distinguishable hits on the detector and works well for both homonuclear and heteronuclear molecular ion beams. The HD^+ molecular ion has been chosen as a simple example to demonstrate the method.

The HD^+ dissociation pathways are: (a) $HD^+ \rightarrow H^+ + D$ and (b) $HD^+ \rightarrow H + D^+$, while ionization leads to (c) $HD^+ \rightarrow H^+ + D^+$. Ionization can be eliminated by reducing the laser intensity below the ionization appearance intensity. This reduces the number of rate equations one has to solve; however, the same method can be used even if ionization occurs.

Let ε_H , ε_D , ε_{H^+} , and ε_{D^+} be the efficiencies for detecting the H, D, H^+ , and D^+ fragments, respectively. Then, we can express the measured number of coincidences and detected hits as follows:

$$M_{H^+D} = \varepsilon_{H^+}\varepsilon_D N_{H^+D}, \quad (1)$$

$$M_{H^+} = \varepsilon_{H^+} N_{H^+D}, \quad (2)$$

$$M_{HD^+} = \varepsilon_H \varepsilon_{D^+} N_{HD^+}, \quad (3)$$

$$M_{D^+} = \varepsilon_{D^+} N_{HD^+}, \quad (4)$$

$$M_{HD} = M_H + M_D = \varepsilon_H N_{HD^+} + \varepsilon_D N_{H^+D}. \quad (5)$$

N_{H^+D} and N_{HD^+} are the total number of true hits in channels (a) and (b), respectively. In order to solve these equations the number of unknowns has to be reduced to five. This is accomplished by assuming that $H^+ + D$ and $H + D^+$ dissociation channels are equally likely, i.e., $N_{H^+D} = N_{HD^+}$. It has been shown that the deviation from this equality is small and occurs only for dissociation with kinetic energy release of a few milli-electron-volts.³² The typical kinetic energy release in laser-induced dissociation is much higher, thus resulting in equal yields in both dissociation channels. We have solved the above equations to get the expressions for the efficiencies as follows. On dividing Eq. (1) by Eq. (2) we get

$$\varepsilon_D = \frac{M_{H^+D}}{M_{H^+}}. \quad (6)$$

Dividing Eq. (3) by Eq. (4) yields

$$\varepsilon_H = \frac{M_{HD^+}}{M_{D^+}}. \quad (7)$$

In a similar way, the expression for the other efficiencies and total number of hits can be written as

$$\varepsilon_{H^+} = \frac{M_{H^+}}{N_{H^+D}} = \frac{M_{HD^+}M_{H^+} + M_{H^+D}M_{D^+}}{M_{HD^+}M_{D^+}}, \quad (8)$$

$$\varepsilon_{D^+} = \frac{M_{D^+}}{N_{H^+D}} = \frac{M_{HD^+}M_{H^+} + M_{H^+D}M_{D^+}}{M_{HD^+}M_{H^+}}, \quad (9)$$

and

$$N_{H^+D} = \frac{M_{HD}}{\varepsilon_H + \varepsilon_D} = \frac{M_{HD}M_{D^+}M_{H^+}}{M_{HD^+}M_{H^+} + M_{H^+D}M_{D^+}}. \quad (10)$$

Similar rate equations for the dissociation of homonuclear molecular ions (e.g., H_2^+) can be written. As these molecular ions dissociate through a single channel $H_2^+ \rightarrow H^+ + H$, we have only three equations and three unknowns. Therefore, no additional assumptions are needed in contrast to the heteronuclear molecular-ion beam case. Furthermore, the algebra leading to ε_H , ε_{H^+} , and N_{HH^+} is simpler than for HD^+ , yielding

$$\varepsilon_H = \frac{M_{HH^+}}{M_{H^+}}, \quad (11)$$

$$\varepsilon_{H^+} = \frac{M_{HH^+}}{M_H}, \quad (12)$$

and

$$N_{HH^+} = \frac{M_H M_{H^+}}{M_{HH^+}}. \quad (13)$$

IV. EXAMPLES

We have obtained the absolute total detection efficiency and also the individual signal detection efficiency for different species resulting from multiphoton dissociation of the HD^+ molecular ion. The absolute total detection efficiency for each fragment is plotted as a function of incident beam energy in Fig. 3(a). The absolute total efficiency is around 20%, which is less than the open area ratio of the detector (i.e., $\sim 50\%$). Similarly, the individual signal absolute detection efficiency for each fragment is plotted as a function of incident beam energy in Fig. 3(b). The individual signal efficiency is around 30%. This detection efficiency is fairly low as expected for the low bias voltage used to demonstrate our method⁹⁻¹³ (see Sec. I). The absolute total efficiency is somewhat lower than the individual signal efficiency because it requires the presence of all signals. It is much larger than the product of the individual efficiencies indicating that the individual signal efficiencies are correlated with each other.

The results above indicate that the timing signal has lower efficiency in comparison to the position signals. Among the position signals the D signal has the lowest efficiency. The lower detection efficiency for D^+ ions is most

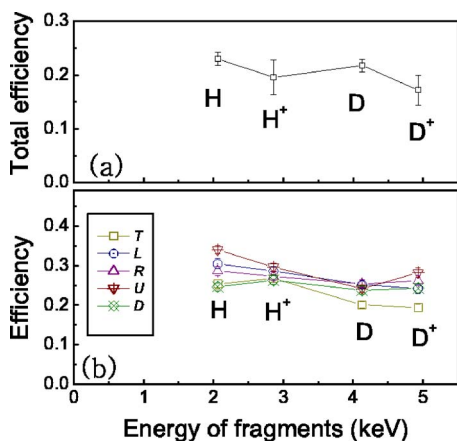


FIG. 3. (a) Absolute total detection efficiency of the detector as a function of fragment energy. (b) The absolute detection efficiency of individual signals as a function of fragment energy. The error bars are the statistical errors.

likely due to the losses caused by the small Faraday cup as these ions are deflected off the beam axis the least in our setup.

The detection efficiency can be improved by changing parameters such as the bias voltage on the detector or the particle impact energy. Below we will show how our method provided the needed feedback to quantify the effect of these changes. First, we used a 7 keV O_2^+ beam with spectrometer voltage of 0.8 kV, which corresponds to a fragment impact energy of 3.18 keV for O and 3.82 keV for O^+ . Then, we increased the detector voltage by 20 V, adjusted the low level discriminator voltage,⁴ and increased the beam energy. After the changes we had an 8 keV O_2^+ beam with a spectrometer voltage of 1.3 kV, which corresponds to a fragment impact energy of 3.48 keV for O and 4.52 keV for O^+ . The efficiencies before and after the modifications are referred to as old and new efficiencies, respectively. The ratio of these absolute detection efficiencies as a function of old efficiency is shown in Fig. 4. The improvement in the detection efficiency of each signal is higher than 10%. This increase in detection efficiency is mostly due to the higher bias voltage as demonstrated in previous work (see, for example, Refs. 9–13). It is important to note the useful feedback provided by our method which can be used to improve the detector efficiency. More importantly, it allows one to identify which of the many detector signals is the main cause for the lower efficiency, thus reducing the guess work in this process.

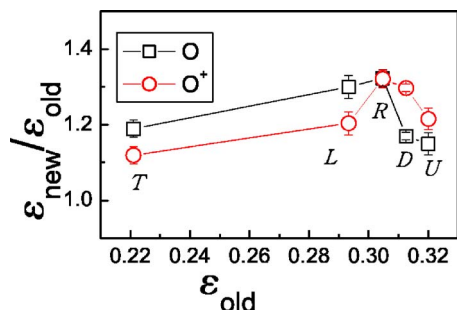


FIG. 4. Ratio of new to old detection efficiencies as a function of old efficiency for individual signals (see text). Note that the order of O_2^+ signal efficiencies differs from those for HD^+ .

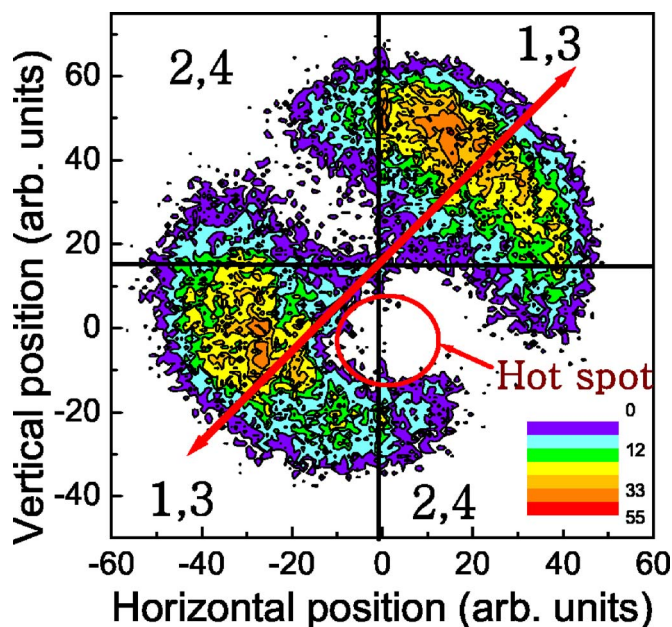


FIG. 5. Position of the H^+ and H hits on the detector and division of the detector into sectors. Note that the dissociation is preferentially along the laser polarization which is rotated by about an angle of 43° relative to the delay line anode. The thick arrow indicates the laser polarization direction.

The position dependent efficiency for a certain area of the detector can be evaluated by dividing the detector into sectors or rings in such a way that the ions which obey momentum conservation will be counted properly. To demonstrate this, we have measured the position dependent efficiency using two sectors. The first and the third quadrants constitute one sector (1,3) while the second and the fourth quadrants constitute the other sector (2,4) as shown in Fig. 5. We have used the data for the dissociation of the H_2^+ molecular ion for this purpose. The detection efficiency of one sector (1,3) for H^+ and H is $\epsilon_{H^+}=0.263\pm 0.001$ and $\epsilon_H=0.251\pm 0.001$, while for the other sector (2,4), $\epsilon_{H^+}=0.214\pm 0.001$ and $\epsilon_H=0.189\pm 0.001$ (here the error bars are smaller because of much better statistics in the H_2^+ data set). This implies that the absolute detection efficiency for one sector is slightly higher than for the other sector for the experimental data set we used as an example. This is due to a hot spot caused by a high impact rate of scattered beam particles, which increases the detector dead time and reduces the efficiency in that spot. This hot spot can be seen in Fig. 5, which is the image of the position of the H^+ and H (gated by

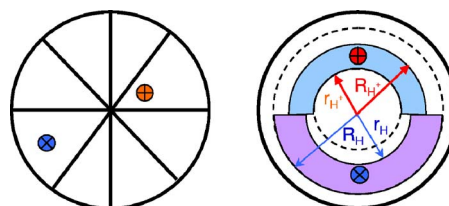


FIG. 6. Schematic division of detector for position dependent efficiency using sectors (left) and rings (right). The \oplus and \otimes represent H^+ and H hits, respectively. The ring of H^+ is indicated by the thick arrowhead and that of H by the thin arrowhead.

their TOF) hits on the detector. The method presented allows one to quantify the reduction in efficiency due to the observed hot spot.

The position dependent efficiency can also be measured by dividing the detector into rings. Care should be taken in this case to define the rings such that the charged fragment H^+ and the neutral H correspond to the rings that contain fragments associated by momentum conservation as shown in Fig. 6. Note that this condition is easy to satisfy for sectors. However, for rings, the ring of H^+ with inner and outer radii r_{H^+} and R_{H^+} has to be somewhat smaller than that of H with radii r_H and R_H due to the effect of the spectrometer field.

V. SUMMARY

We have presented a method for the direct measurement of the absolute detection efficiency of a detector. This method is applicable to any type of particle detector as long as the particle breakup results in two distinguishable hits on the detector. It gives a direct measurement of the absolute detection efficiency for both total and individual (i.e., timing and position) signals. It also helps to identify inefficient signals. Further, we have demonstrated how the immediate quantitative feedback provided by this method can be applied to improve the detector efficiency significantly. Finally, the method can be used to compare the absolute detection efficiency of different sections of the position decoding anode and also to quantify the reduction in efficiency (and hence the statistics) due to hot spots in certain regions of the detector.

ACKNOWLEDGMENTS

The authors acknowledge Zenghu Chang for providing the laser beams and C. Fehrenbach for technical help. This work was supported by the Chemical Sciences, Geosciences and Biosciences Division, Office of Basic Energy Sciences, Office of Science, U.S. Department of Energy.

¹R. Dörner, V. Mergel, O. Jagutzki, L. Spielberger, J. Ullrich, R. Moshhammer, and H. Schmidt-Böcking, *Phys. Rep.* **330**, 95 (2000).

²J. Ullrich, R. Moshhammer, A. Dorn, R. Dörner, L. Ph. H. Schmidt, and H. Schmidt-Böcking, *Rep. Prog. Phys.* **66**, 1463 (2003).

³D. Céolin, G. Chaplier, M. Lemonnier, G. A. Garcia, C. Miron, L. Nahon, M. Simon, N. Leclercq, and P. Morin, *Rev. Sci. Instrum.* **76**, 043302

(2005).

⁴Y. Zhang, H. J. Whitlow, T. Winzell, I. F. Bubbs, T. Sajavaara, K. Arstila, and J. Keinonen, *Nucl. Instrum. Methods Phys. Res. B* **149**, 477 (1999).

⁵H. O. Funsten, R. W. Harper, and D. J. McComas, *Rev. Sci. Instrum.* **76**, 053301 (2005).

⁶E. A. Kurz, *Am. Lab. (Shelton, Conn.)* **11**, 67 (1979), and references therein.

⁷A. J. Guest, *Acta Electron.* **14**, 79 (1971).

⁸D. H. Crandall, J. A. Ray, and C. Cisneros, *Rev. Sci. Instrum.* **46**, 562 (1975).

⁹J. L. Wiza, *Nucl. Instrum. Methods* **162**, 587 (1979), and references therein.

¹⁰H. C. Straub, M. A. Mangan, B. G. Lindsay, K. A. Smith, and R. F. Stebbings, *Rev. Sci. Instrum.* **70**, 4238 (1999).

¹¹R. S. Gao, P. S. Gibner, J. H. Newman, K. A. Smith, and R. F. Stebbings, *Rev. Sci. Instrum.* **55**, 1756 (1984).

¹²R. R. Goruganthu and W. G. Wilson, *Rev. Sci. Instrum.* **55**, 2030 (1984).

¹³L. Lundin and U. Rolander, *Appl. Surf. Sci.* **67**, 459 (1993).

¹⁴E. Lienard, M. Herbane, G. Ban, G. Darius, P. Delahaye, D. Durand, X. Flechar, M. Labalme, F. Mauger, A. Mery, O. Naviliat-Cuncic, and D. Rodriguez, *Nucl. Instrum. Methods Phys. Res. A* **551**, 375 (2005).

¹⁵B. Brehm, J. Grosser, T. Ruschinski, and M. Zimmer, *Meas. Sci. Technol.* **6**, 953 (1995).

¹⁶J. Oberheide, P. Wilhelms, and M. Zimmer, *Meas. Sci. Technol.* **8**, 351 (1997).

¹⁷A. Müller, N. Djurić, G. H. Dunn, and D. S. Belić, *Rev. Sci. Instrum.* **57**, 349 (1986).

¹⁸T. M. Stephen and B. L. Peko, *Rev. Sci. Instrum.* **71**, 1355 (2000).

¹⁹J. A. Panitz and J. A. Foesch, *Rev. Sci. Instrum.* **47**, 44 (1976).

²⁰G. W. Fraser, *Nucl. Instrum. Methods Phys. Res.* **206**, 445 (1983).

²¹T. Sakurai and T. Hashizume, *Rev. Sci. Instrum.* **57**, 236 (1986).

²²B. Deconihout, F. Vurpillot, and M. Bout, *Rev. Sci. Instrum.* **73**, 1734 (2002).

²³B. Deconihout, P. Gerard, M. Bout, and A. Bostel, *Appl. Surf. Sci.* **94–95**, 422 (1996).

²⁴H. O. Funsten, D. M. Suszcynsky, R. W. Harper, J. E. Nordholt, and B. L. Barraclough, *Rev. Sci. Instrum.* **67**, 145 (1996).

²⁵R. C. Taylor, M. C. Hettrick, and R. F. Malina, *Rev. Sci. Instrum.* **54**, 171 (1983).

²⁶I. Ben-Itzhak, P. Q. Wang, J. F. Xia, A. M. Sayler, M. A. Smith, J. W. Maseberg, K. D. Carnes, and B. D. Esry, *Nucl. Instrum. Methods Phys. Res. B* **233**, 56 (2005).

²⁷P. Q. Wang, J. F. Xia, A. M. Sayler, M. A. Smith, K. D. Carnes, B. D. Esry, and I. Ben-Itzhak, *Phys. Rev. A* **74**, 043411 (2006).

²⁸G. Da Costa, F. Vurpillot, A. Bostel, M. Bouet, and B. Deconihout, *Rev. Sci. Instrum.* **76**, 013304 (2005).

²⁹P. G. Friedman, R. A. Cuza, J. R. Fleischman, C. Martin, D. Schiminovich, and D. J. Doyle, *Rev. Sci. Instrum.* **67**, 596 (1996).

³⁰O. Jagutzki, A. Cerezo, A. Czasch, R. Dörner, M. Hattab, M. Huang, V. Mergel, U. Spillmann, K. Ullmann-Pfleger, T. Weber, H. Schmidt-Böcking, and G. D. W. Smith, *IEEE Trans. Nucl. Sci.* **49**, 2477 (2002).

³¹Detector details can be found at www.roentdek.com

³²E. Wells, K. D. Carnes, B. D. Esry, and I. Ben-Itzhak, *Phys. Rev. Lett.* **86**, 4803 (2001).